Improvisations in phototrophy. Protein engineering and functional investigation of rhodopsin proton-pumps

Ganapathy, S.

Chapter 3

Retinal based proton pumping in the near-infrared

Shifting the action spectra of rhodopsin proton-pumps beyond 700 nm would generate many new prospects in optogenetics, membrane sensor technology, and complementation of oxygenic phototrophy. We thereby studied the effect of red-shifting analogs of retinal, combined with red-shifting mutations, on the spectral properties and pump activity of proteorhodopsins. We investigated a variety of analogs, of which the novel analog 3-methylamino-16-nor-1,2,3,4-didehydroretinal (MMAR), produced exciting results. This analog red-shifted all rhodopsin variants tested, accompanied by a strong broadening of the absorbance band, tailing out to 850-950 nm. In particular, MMAR showed a strong synergistic effect with the PR-D212N,F234S double mutant, inducing an astonishing 200 nm red-shift in the absorbance maximum, which is by far the largest red-shift reported for any retinal protein. Very importantly, all MMAR containing holoproteins are the first rhodopsins retaining significant pump activity under near-infrared illumination (730 nm). Such MMAR-based rhodopsin variants present very promising opportunities for further synthetic biology modification and for a variety of biotechnological and biophysical applications.

This chapter has been published as: S. Ganapathy, H. Venselaar, Q. Chen, H. J. M. de Groot, K. J. Hellingwerf, W. J. de Grip **(2017)** *Journal of the American Chemical Society* 139 (6): 2338-2344

3.1 Introduction

In chapter 2 we confirm that PR and GR can be easily expressed in good yields in a non-native host like *Escherichia coli.* We further show that they can be readily combined with retinal analogs to generate analog pigments with different spectral properties, while maintaining pump activity. In addition, retinal analog induced spectral shifts can be additive to spectral shifts induced by mutagenesis. Such features make PR and GR attractive model systems for synthetic biology applications. A challenge in many of these applications is to extend the action spectrum of rhodopsins into the far-red and near-infrared (NIR) range of the electromagnetic spectrum (≥700 nm), which is relatively unexplored and has many advantages [1]. In chapter 2, the retinal analog A2 (Figure 3.1) was identified as a red-shifting analog, which retained significant activity of the corresponding pigments. In this chapter, we specifically focus on red-shifting retinal analogs containing more extensive ring modifications. We extend the conjugation of A2 by adding electron withdrawing substituents at the C3 position on the β-ionone ring. Here, we report on the ring-modified analogs: all-*trans*-3-methoxy-3,4-dehydroretinal (MOA2), all-*trans*-3-dimethylamino-16-nor-1,2,3,4-didehydroretinal (DMAR) and all-*trans*-3-methylamino-16-nor-1,2,3,4-didehydro retinal (MMAR) (Figure 3.1). MOA2 was shown before to red-shift visual rhodopsins up to 130 nm with retention of activity [2]. DMAR was based upon a 3-dimethylaminophenyl derivative of retinal, lacking methyl groups in the aromatic ring, which red-shifted channelrhodopsin 2 by 40 nm, while maintaining a retarded photocycle [3]. MMAR we devised on the basis of the results we obtained with DMAR. These analogs were combined with WT PR and GR as well as with the red-shifted mutants PR-D212N, F234S (PR-DNFS), PR-T101A (PR-TA) and GR-F260S (GR-FS) (Figure 3.2).

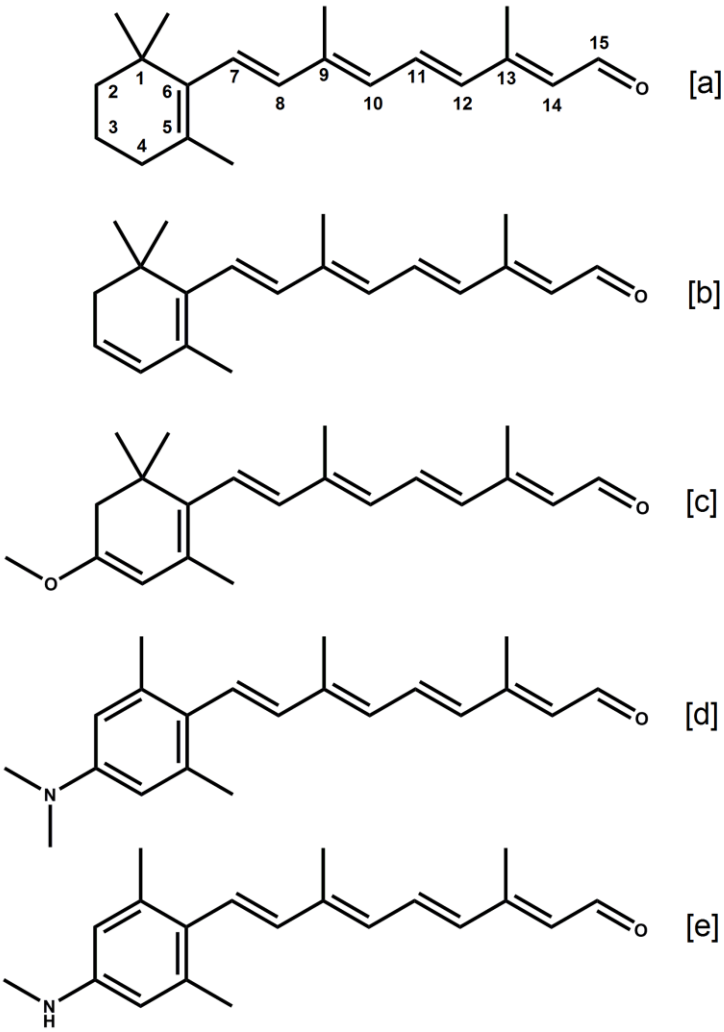

Figure 3.1 Chemical structures of retinal analogs used in this chapter [a] A1 [b] A2 [c] MOA2 [d] DMAR [e] MMAR. For nomenclature and spectral properties see Introduction and Appendix (Figure A2.1).

While all analogs tested yielded red-shifted pigments, MMAR was finally identified as the most promising analog from our study, inducing bathochromic shifts up to an astonishing 200 nm, while retaining activity in near-infra red light. MMAR pigments have broad potential for a variety of biotechnological, optogenetic and oxyphototrophic applications.

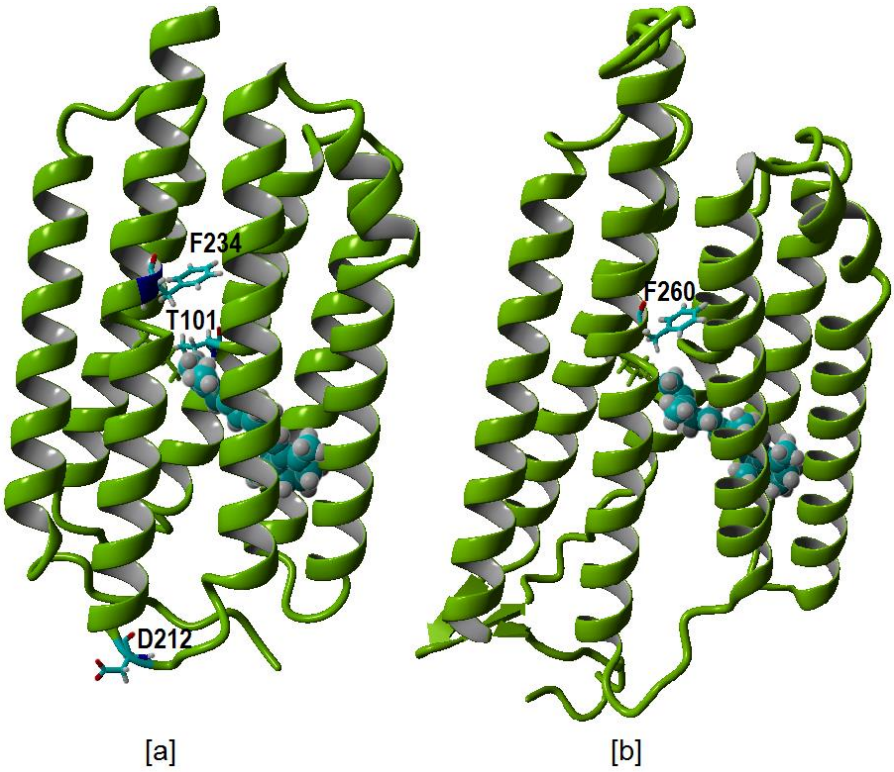

Figure 3.2 [a] Homology model of PR selectively displaying the mutation sites in cyan: F234 and T101 near the retinal binding pockets; and D212 in the loop region. [b] Homology model for GR selectively displaying the mutation site F260 in cyan, in the retinal binding pocket. The retinylidene chromophore is represented in cyan as a space-filled residue.

3.2 Experimental section

Next to the materials and methods already described in Chapter 2, the following materials and methods were used in this chapter.

3.2.1 Materials

All-*trans*-3,4-dehydroretinal (A2) was a generous gift from Hoffman-LaRoche. All-*trans*-3-methoxy-3,4-dehydroretinal (MOA2; purity 97.8% according to the manufacturer's certificate of analysis), all-*trans*-3-dimethylamino-16-nor-1,2,3,4-didehydroretinal (DMAR; purity 99.9%)

and all-*trans*-3-methylamino-16-nor-1,2,3,4-didehydroretinal (MMAR; purity > 99.9%) were synthesized on order by Buchem, B.V. (Apeldoorn, The Netherlands).

3.2.2 Spectroscopy of membrane vesicles:

The spectral properties of the pigments were measured in intact membrane vesicle suspensions using the end-on spectrophotometer SPECORD 210 PLUS (Analytik Jena). The end-window configuration of the photomultiplier and a close distance to the cuvette reduces the loss of light due to scattering by the vesicles. To isolate the major absorbance band of the proteorhodopsin out of the composite spectrum of membrane vesicles, hydroxylamine was added from a 1 M stock solution, pH 7, to a final concentration of 50 mM, followed by illumination with white light for 10 minutes. Hydroxylamine attacks the Schiff base and releases the retinal from the opsin binding pocket as retinaloxime. A difference spectrum then reveals the major absorbance band of the proteorhodopsin present. The same protocol was also used after solubilization of membrane vesicles with DDM. The vesicle protocol and DDM protocol were compared with pigments that were stable in DDM, and yielded equivalent results ($\pm$ <5%).

3.2.3 Spectroscopy of purified protein:

In order to test the pH-dependence of the main absorbance band of the PR based pigments, the purified proteins were analysed at different pH values by diluting the samples 1:1 with buffers containing either 100 mM bis-tris-propane at pH 9, 8.5, 8, 7.5, 7, 6.5, 6 or 100 mM MES at pH 5.5 or 5. For determination of molar absorbance values the purified pigments based upon WT PR and GR were illuminated in DDM (pH 7) in the presence of hydroxylamine as described in Chapter 2. The maximum absorbance of the generated oxime derivatives was measured, and was used to calculate the molar absorbance values of the corresponding WT PR and GR pigments.

3.2.4 Molar absorbance of retinals and corresponding pigments:

The λ_{max} (nm) and molar absorbance ε ($M^{-1}.cm^{-1}$) for A1, A2, MOA2, DMAR and MMAR and their corresponding oximes are listed in the appendix (Table A.2.2). In order to calculate the ε values, a stock solution of the retinals was made containing 1 mg of the crystalline powder dissolved in 1 ml of DMF, and its absorbance was measured using appropriate dilutions. Beer-Lambert's law was used to calculate the ε of the analogs in DMF. An aliquot of this stock was diluted 1:100 with a solution containing 1% DDM in 10 mM Tris pH 7, to determine the corresponding ε of the analogs in DDM. Hydroxylamine was then added to the DMF and DDM solutions to a final concentration of 50 mM and the solution was illuminated. The absorbance spectra of the resulting retinal oximes were measured and used to calculate the ε in DMF and DDM. These measurements were done in duplicate, resulting in a S.D. ≤ 8%. The ε of the oximes of A1 and A2 were previously calculated to be 51700 $M^{-1}.cm^{-1}$ at λ_{max}=367 nm and 45400 $M^{-1}.cm^{-1}$ at λ_{max}=386 nm respectively in 1% digitonin solution [4-6]. Based on our measurements, we calculated ε of 52500 $M^{-1}.cm^{-1}$ at λ_{max}=368 nm and 44000 $M^{-1}.cm^{-1}$ at λ_{max}=385 nm for A1 and A2 oximes in 1% DDM, respectively, in good agreement with the literature values. The ε values for the WT PR and GR pigments, calculated from the corresponding oxime absorbance, are also listed in Table A.2.2. The molar absorbances of PR:A1 and GR:A1 in detergent solution were estimated before. Our ε=55500 $M^{-1}.cm^{-1}$ for GR:A1 is not significantly different from the reported value of 50000 [7]. Our ε=54200 $M^{-1}.cm^{-1}$ for PR:A1 is however significantly larger than the earlier reported ε=44000 $M^{-1}.cm^{-1}$ [8]. Considering the reported molar absorbances for bacteriorhodopsin (54000 [9] and 63000 $M^{-1}.cm^{-1}$ [10]), we decided to keep to our own higher values for both PR and GR.

3.2.5 Proton pumping assay:

Suspensions of starved cells were generated as described in Chapter 2, section 2.2.9. The following light sources were used: white light (DLED9-T,

DEDOLIGHT; 800 $\mu E.m^{-2}.s^{-1}$); 617 nm LED (M617L3, Thorlabs; 1500 $\mu E.m^{-2}.s^{-1}$); 660 nm LED (M660L4, Thorlabs; 800 $\mu E.m^{-2}.s^{-1}$); 730 nm LED (M730L4, Thorlabs; 150 $\mu E.m^{-2}.s^{-1}$). Light-induced pH changes were measured with a pH microelectrode (SenTix MIC, WTW) and the readout was monitored by a pH meter (Inolab pH 7310, WTW) connected to a computer. The following light regime was used: 1 min dark, 1 min light, 2 min dark, 1 min light, 2 min dark. For the 730 nm illumination of all species and 660 nm illumination for PR-DNFS, a longer illumination period of 1.5 min was used, along with a 2 x concentrated cell suspension (cells from 50 mL culture in 4 mL starvation buffer). Pumping rates were calculated using two independent trials. A calibration curve was measured using 0.1 M HCl and 0.1 M oxalic acid. Pumping rates were calculated as protons/sec from the initial rate of the light-induced pH change, if required corrected for baseline drift in controls (starved cells without expression of proteo-opsin or without retinal). Molecular pumping rates could subsequently be calculated after assay of the proteorhodopsin level.

3.2.6 Determination of proteorhodopsin levels:

The above cell suspension from the proton pumping assay was rinsed with starvation buffer and the pellet was resuspended in 10 mL buffer B (50 mM Tris-HCl, 150 mM NaCl, pH 7). The cell suspension was sonicated as mentioned above and the membrane vesicles and cell debris were pelleted together (147,000xg, 4°C, 1 h). The pellet was resuspended in 4 mL of buffer B. An aliquot of this membrane vesicle suspension was used to extract the main absorbance band of the analog pigments after bleaching with hydroxylamine, using the end-on spectrophotometer. This method was useful to estimate the concentration of analog pigments which were unstable in DDM, particularly GR:DMAR, GR:MMAR, GR-FS:MMAR and PR-TA:MMAR. To another aliquot of the membrane vesicle suspension, DDM was added to a final concentration of 2.5% and incubated at RT with mixing overnight. Under these conditions maximum extraction of all stable

pigment species was achieved without significant losses. The following day, the insoluble material was removed by centrifugation at 16,000xg, 4°C for 20 min. The supernatant was used to measure an absorbance spectrum before and after bleaching with hydroxylamine. The optical density at the absorbance maximum was used to calculate the original proteorhodopsin level in the cell suspension, using the calculated ε listed in the Appendix, Table A.2.2. Hereby we assumed that the molar absorbance of the mutants is not significantly different from the parent pigments.

3.3 Results

3.3.1 Selection and properties of retinal analogs

In Chapter 2, we observed that A2 induced significant red-shifts in all species tested while largely retaining pump activity. In this chapter, we elaborated the conjugation of A2 by adding different electron withdrawing substituents at the C3 position in the β-ionone ring and/or at C13 or C14 in the polyene chain. Analogs modified at C13 or C14, however, showed poor reactivity or low stability of the resulting holoprotein (see Appendix A.4). Here, we report on the ring-modified analogs MOA2, DMAR and MMAR (Figure 3.1).

MOA2 contains the strong electron withdrawing methoxy group at the C3 position on the β-ionone ring. An extensive π-system is delocalized over the lone pairs of electrons on the oxygen atom of MOA2, resulting in a large red-shift of 52 nm relative to A1 (λ_{max} 434 nm vs 378 nm in DMF) along with a broadening of the main absorbance band (see Appendix, Figure A.2.1). DMAR contains an aromatized β-ionone ring with a bulky dimethylamino group at the C3 position. This analog was modelled on a variant lacking methyl groups on the β-ionone ring [3]. In Chapter 2, we showed that the aromatic PHE, which lacked methyl groups on the ring, did not form a stable pigment with GR [11]. Therefore, we decided to position

methyl groups, which are known to stabilize the retinal inside the binding pocket [12, 13], at the C1 and C5 positions, resulting in DMAR.

However, during the course of our study, we discovered that DMAR formed unstable pigments, which had low pumping activity. We surmised that the bulky dimethylamino group probably sterically hindered the fit and stability of DMAR in the retinal binding pocket. Considering that MOA2 containing a methyl-oxo substitution at C3 smoothly incorporates in all opsins, we therefore conceived MMAR, which contains only a single methyl group on the C3-amino substituent. This modification does not affect the absorbance of the free retinal analog in DMF, as both DMAR and MMAR display a similar complex absorbance band with a λ_{max} at ~434 nm, and an electronic side band at 360 nm (see Appendix, Figure A.2.1). However, when bound to the proteo-opsins, MMAR provides a definite increase in stability and proton pumping activity, compared to DMAR.

3.3.2 Expression and characterization of pigments

In the previous chapter we also described the generation of the PR double mutant PR-DNFS using mis-match PCR. Analogous to the single mutation in F234S in PR, we introduced the equivalent mutation in GR (F260S), based upon homology modeling (Figure 3.2). GR-FS only shows a small red-shift (9 nm), but in contrast to PR-DNFS retains full activity. We further generated PR-TA (T101A, Figure 3.2) [14]. This mutation introduces a 16 nm red-shift while maintaining significant pump activity. Several other single mutations and combinations were generated, but these displayed relatively smaller additional red-shifts with strong loss of pumping activity (Appendix A.5).

PR, GR and the mutants PR-DNFS, PR-TA and GR-FS were recombinantly expressed in *E. coli* strain UT5600 as described in Chapter 2. All opsins could be fully regenerated with A1 and A2, either upon addition of retinal

to the cell culture, or in isolated membrane vesicles. Good regeneration rates were also observed with MOA2 and MMAR, but complete regeneration with DMAR was difficult to achieve. The pigments were further purified using the C-terminal 6x-His tag to a high degree of purity in DDM. However, all the DMAR species and certain MMAR pigments (namely GR, GR-FS, and PR-TA) were not very stable in DDM, which was problematic for the estimation of expression levels. We found a way around this, by measuring the pigment absorbance in intact membrane vesicles.

The main absorbance bands of the pigments in membrane vesicles or in a solubilized state were extracted by reaction with hydroxylamine during illumination to liberate the bound retinal by converting it into the corresponding oxime. This reaction in membrane vesicles was particularly useful to extract the absorbance bands of pigments which were not sufficiently stable in DDM, or which could not survive the purification process. Furthermore, the oxime production was used to determine the molar absorbance values of the various analog species. This allowed quantification of expression levels, and thereby molecular pumping rates for all species generated.

The proton pumping activity of all analog species was measured using four different illumination conditions, namely white light (spectral range 300-900 nm), 617 nm LED (600-640 nm), 660 nm LED (620-680 nm) and 730 nm LED (690-760 nm) illumination. We used intact *E. coli* cells which were starved for an optimum duration of 4 days in a minimal buffer, and further incubated in the presence of valinomycin. The rates obtained probably do not yet reflect the maximally attainable ones, since the applied light intensities are still limiting. Hence, due to the variation in the photon flux of the illumination sources used, the pumping rates were normalized within a set of light conditions to the highest pumping activity obtained (Table 3.1). For instance, GR-FS:A1 has the highest pumping rate with white light (9.4

$H^+.s^{-1}$ per protein); hence white light pumping rates of all pigments are normalised to 9.4. For a comparison between the different light regimes, we can further normalize the highest pumping rates obtained in each light regime, to the highest pumping rate under white light illumination. For reference, these values are: White light (GR-FS:A1, 100%); 617 nm (GR-FS:A1, 80% of white light); 660 nm (GR:A2, 15% of white light) and 730 nm (GR-FS:MMAR, 2% of white light).

3.3.3 Properties of A2, MOA2 and DMAR pigments

In chapter 2, we demonstrated a 26-32 nm red shift in the absorbance bands of the A2 pigments of PR, GR and PR-DNFS. This red-shift was also observed with the PR-TA and GR-FS mutants tested in the present chapter (Table 3.1). All A2 species retained strong proton pumping activity upon white light illumination (50-100% of A1), except for PR-DNFS (23%), corroborating the results reported before [11] (Table 3.1). However, under 730 nm illumination, very low but measurable activity was only observed for the A2 pigments of GR and GR-FS (Figures 3.5, 3.6; Table 3.1). MOA2 was previously shown to induce large spectral shifts of up to 130 nm in visual rhodopsins, while retaining their activity [15]. When bound to the various proteo-opsins used in this study, MOA2 also shifts their absorbance bands to significantly longer wavelengths (55-80 nm, Table 3.1). All MOA2 pigments retain around 15-30% proton pumping activity upon white light illumination. However, negligible proton pumping activity of all these species was observed, when excited with lower energy light (617 nm), despite the high photon flux of the LED source used (1500 $\mu E.m^{-2}.s^{-1}$).

DMAR (Figure 3.1) was modelled after a recent publication [3] that employed a variant lacking methyl groups on the β-ionone ring. This resulted in a 40 nm red-shift in the action spectrum of ChR2 accompanied by a slower photocycle. We inferred that additional methyl groups at the ring would improve the stability and activity of such analog pigments.

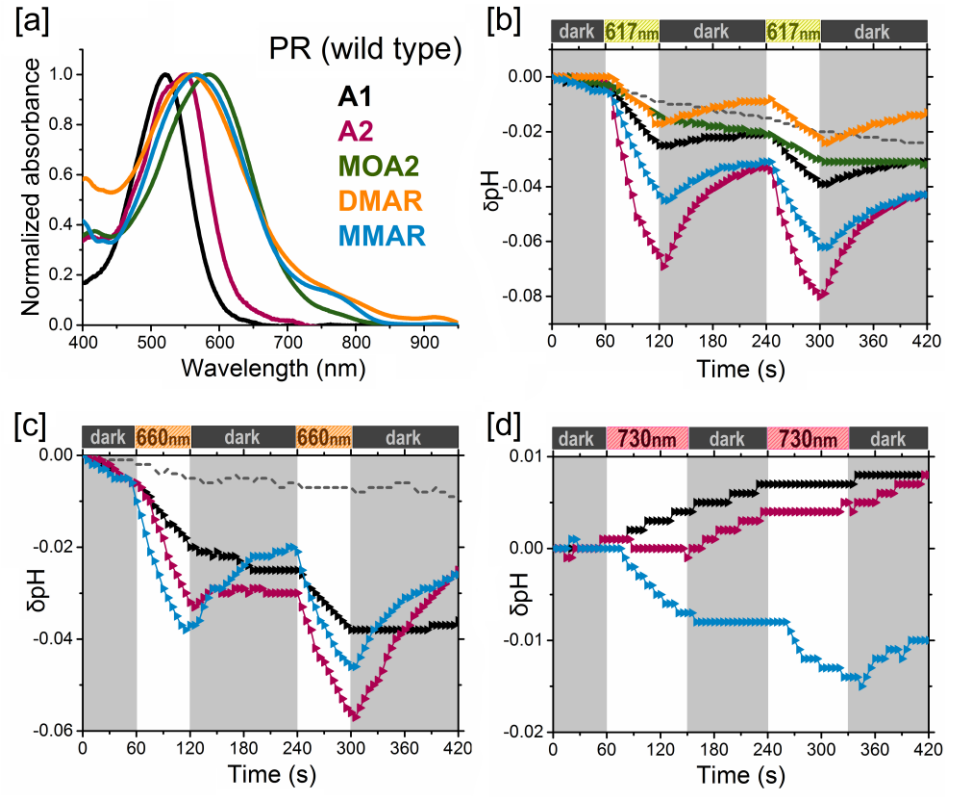

Figure 3.3 Analog pigments of PR. [a] Normalized absorbance spectra of purified pigments in DDM containing A1 (black), A2 (pink), MOA2 (green), DMAR (orange) or MMAR (blue). [b-d] Proton pumping activity of the pigments (same colors) in starved *E. coli* UT5600 cells upon illumination with 617 nm [b], 660 nm [c], and 730 nm [d]. Controls without retinal are represented as a dashed line.

DMAR, however, did not react very smoothly with any of the opsins and a significant red-shift was observed only with PR (38 nm; Table 3.1). Furthermore, DMAR pigments, in particular with GR and GR-FS, were quite unstable in detergent solution. No intact pigment could be isolated for these pigments in DDM, even upon rapid solubilization in the cold (data not shown). The DMAR pigments showed relatively low pumping rates under white light illumination (<10% of A1; Table 3.1, Figure 3.3, 3.5). On the other hand, they could still be activated by 617 nm illumination.

We did not extensively investigate the MOA2 pigments (no pump activity in red light) or the DMAR pigments (poor reactivity and thermal stability). However, the persistent pump activity of DMAR pigments in red light (Table 3.1) led us to elaborate upon this concept and test a variant, MMAR (Figure 3.1). This analog produced exciting results.

3.3.4 Properties of MMAR pigments

MMAR induced a 47 nm red-shift in the λ_{max} of PR and a 23-30 nm red-shift in the λ_{max} of PR-TA, GR and GR-FS (Table 3.1), accompanied with extensive spectral broadening and tailing up to 850-950 nm (Figure 3.3, 3.4, 3.5, 3.6). PR:MMAR also displayed a composite band around 770 nm (Figure 3.3). All PR based pigments exhibited the slight red-shift in the main absorbance band upon acidification (Figure 3.8, panel a). However, in PR:MMAR this was accompanied by an unusual enhancement of the absorbance around 770 nm (Figure 3.8, panel b). In the PR-DNFS:MMAR pigment this enhancement of the lower-energy bands was already induced by the mutation, resulting in an extraordinary red-shift of the absorbance band to ca 740 nm (Figure 3.4). Even then, acidification induced a congruent red-shift with some further enhancement of the 740 band (Appendix, Figure A.5).

All MMAR pigments displayed relatively low proton pumping activity under white light (5-10 % of A1 and A2). However, significant activity was retained with 730 LED illumination, in fact strongly surpassing that of any remaining A2 activity (Figures 3.3, 3.4, 3.5, 3.6; Table 3.1). Because of the low intensity of the 730 LED, an absolute comparison cannot yet be made, but we estimate that under equal intensity light the pumping activity with the 730 LED would be at least as high as under white light. Even the PR-DNFS mutant, which is quite impaired in its pump function (with A1, 30 – 40 % of WT in white light), with MMAR clearly displays pumping activity under 730 LED illumination (Figure 3.4).

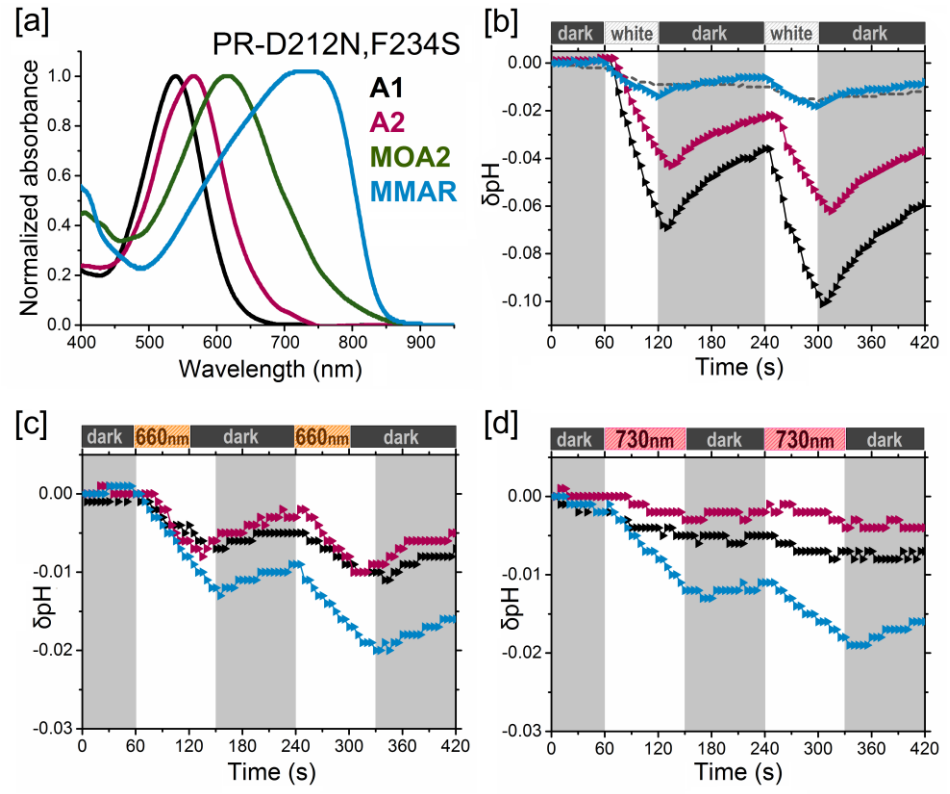

Figure 3.4 Analog pigments of PR-D212N,F234S. [a] Normalized absorbance spectra of purified pigments in DDM containing A1 (black), A2 (pink), MOA2 (green) or MMAR (blue). [b-d] Proton pumping activity of the pigments (same colors) in starved *E. coli* UT5600 cells upon illumination with white light [b], 660 nm [c] and 730 nm [d]. Controls are represented as a dashed line.

The highest activity under this NIR light was observed for the GR-FS:MMAR combination (0.2 $H^+.s^{-1}$ per protein), but this will still increase considerably at higher light intensity and broad frequency-range illumination.

3.4 Discussion

3.4.1 A2, MOA2 and DMAR pigments

All opsin variants tested with MOA2 reacted smoothly forming stable pigments in DDM, allowing extensive purification. MOA2 not only induced very large red-shifts in λ_{max} (55-81 nm, depending on the opsin, Table 3.1), but also increased the half-width of the spectra. As a result, all the spectra tail out clearly beyond 700 nm, up to 800-850 nm (Figures 3.3, 3.4, 3.5, 3.6). Under white light illumination, all MOA2 pigments tested showed low proton-pump activity (15-30% of the corresponding A1 pigments). We expected this ratio to increase in red light, in view of the red-shifted absorbance bands of the MOA2 pigments. However, hardly any pump activity could be detected with 617 nm LED illumination (Table 3.1, Figures 3.3, 3.5). This was a surprising result, since the emission band of the LED overlaps with a significant portion of the main absorbance bands of all MOA2 pigments. The low energy light with $\lambda>600$ nm is apparently insufficient to drive a complete photocycle, and the strong electronegative character of the methoxy substituent may effectively suppresses the pump mechanism. We are currently investigating this phenomenon further by femtosecond spectroscopy and a computational investigation of the energetic constraints involved in photoexcitation of MOA2 pigments.

Subsequently, we turned to the 3-dimethylaminophenyl derivative that maintained activity in the channelrhodopsin ChR2 [3], but decided to add a methyl group at position 1 and 5 to increase fit and stability in the binding site [12]. This resulted in the novel derivative DMAR (Figure 3.1). DMAR, however, showed low reactivity with most opsins and very low stability of the resulting pigments in DDM, especially for GR and GR-FS. Of all pigments tested, only PR:DMAR could be successfully purified (Figure 3.3), showing a broad absorbance band peaking at 558 nm (38 nm red-shift) and extending out to 850 nm. A clue for this discriminatory behaviour can be

extracted from the homology models of PR and GR (Figure 2.5). PR contains a Phe 152 group in the retinal binding pocket, which might stabilize the aromatic ring in DMAR via π-π stacking interactions. GR however contains a G178 in this location and would lack this stabilizing effect.Moreover, the bulky dimethylamino group probably sterically hinders the fit and reactivity of DMAR in the retinal binding pocket. While low pumping rates (<10% of A1) were observed under white light illumination for both PR:DMAR and GR:DMAR, it was inspiring to notice that now pumping persisted under 617 nm illumination (Figures 3.3 and 3.5). Hence, we decided to improve reactivity of this analog and stability of the resulting pigments, by replacing the larger dimethylamino group in DMAR with the smaller monomethylamino group. This group is similar in size to the methoxy group in MOA2, an analog that yields very stable pigments. This strategy resulted in MMAR (Figure 3.1).

3.4.2 MMAR pigments

MMAR indeed rapidly incorporated in all opsins and the resulting pigments showed a clear increase in stability and proton pumping activity, compared to DMAR. MMAR thus came out as the most promising analog identified from our study. MMAR induced bathochromic shifts in all opsins tested, along with broadening of the absorbance bands. However, the unprecedented ~200 nm shift (equivalent to 5005 cm^{-1}) in the absorbance of PR-DNFS:MMAR relative to the A1 pigment is a spectacular result from this chapter, which is discussed in more detail, below.

PR-derived pigments exhibit a 20-30 nm red-shift in the main absorbance band (Figure 3.8) upon protonation of the counterion (D97; pKa ~6.5). Of all PR pigments, only PR:MMAR displayed a complex absorbance band with a λ_{max} at 567 nm containing a 770 nm composite band, which extends to 850 nm (Figure 3.3).

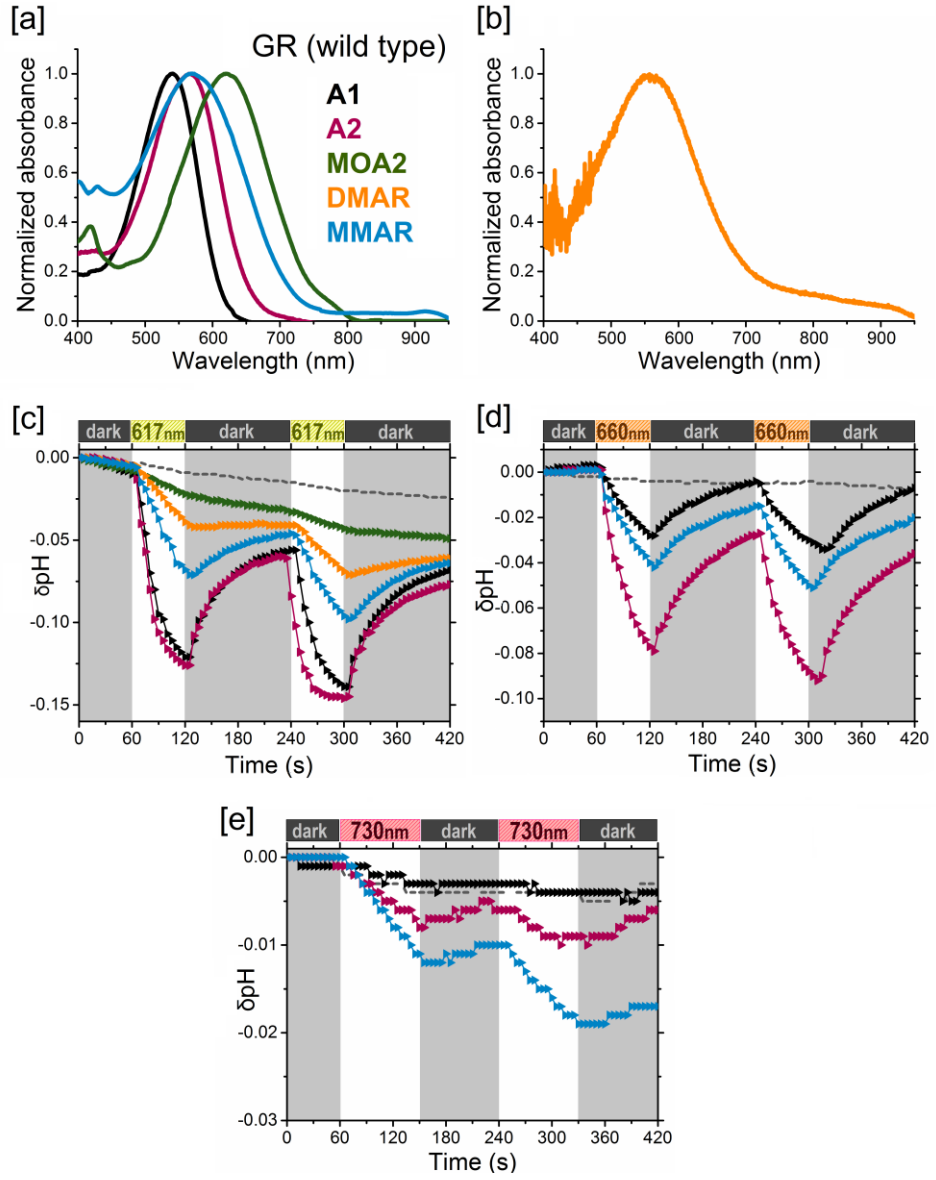

Figure 3.5 Analog pigments of GR [a] Normalized absorbance spectra of His-tag purified pigments in DDM containing A1 (black), A2 (pink), MOA2 (green) or MMAR (blue). [b] Hydroxylamine difference spectra of the DMAR pigment (orange) in membrane vesicles. [c-e] Proton pumping activity of the pigments (same colors) in starved *E. coli* UT5600 cells upon illumination with 617 nm [c], 660 nm [d], and 730 nm [e]. Controls are represented as a dashed line.

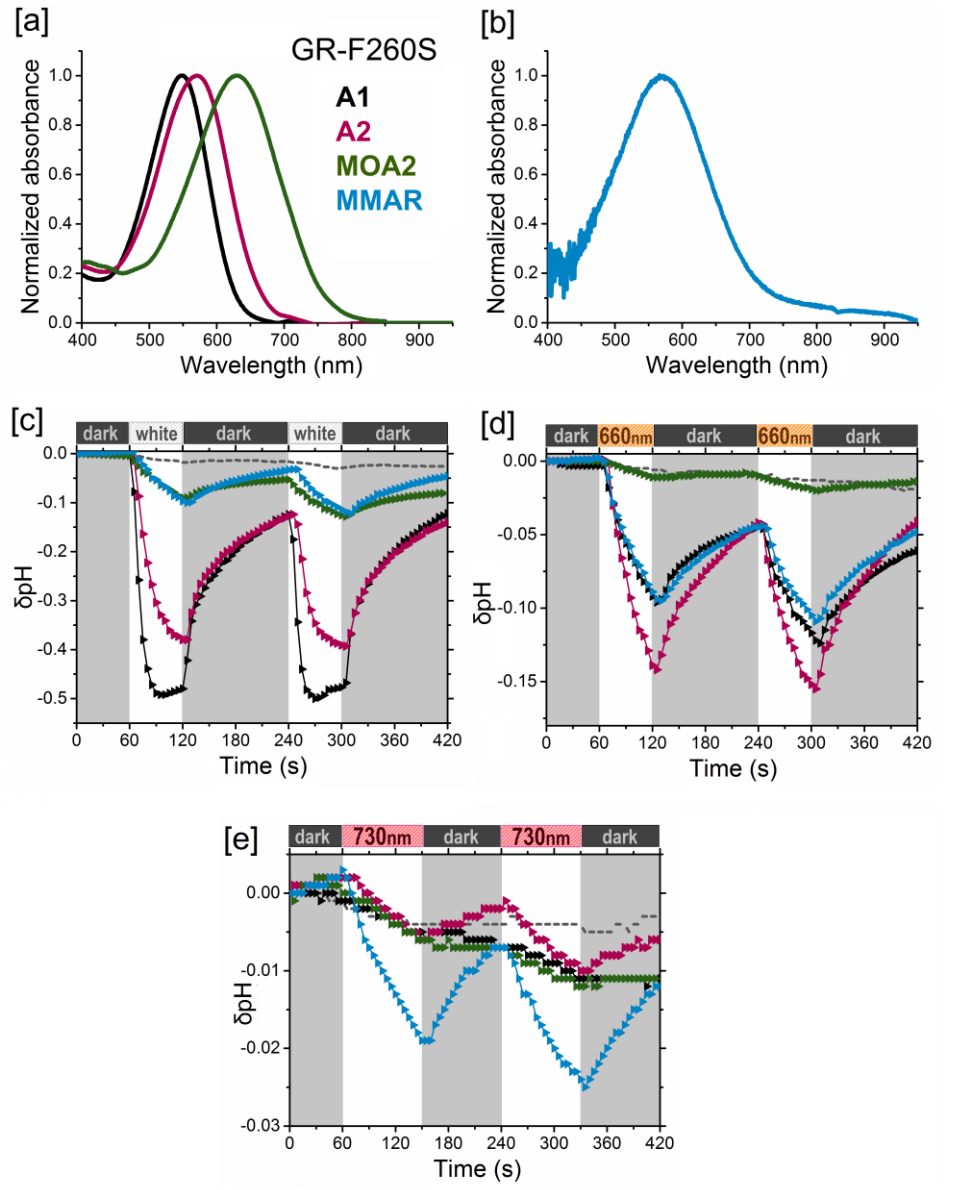

Figure 3.6 Analog pigments of GR-F260S [a] Normalized absorbance spectra of His-tag purified pigments in DDM containing A1 (black), A2 (pink) and MOA2 (green). [b] Hydroxylamine difference spectrum of the MMAR pigment (blue) in membrane vesicles. [c-e] Proton pumping activity of the pigments (same colors) in starved E. coli UT5600 cells upon illumination with white light [c], 660 nm LED [d] and 730 nm LED [e]. Controls are represented as a dashed line.

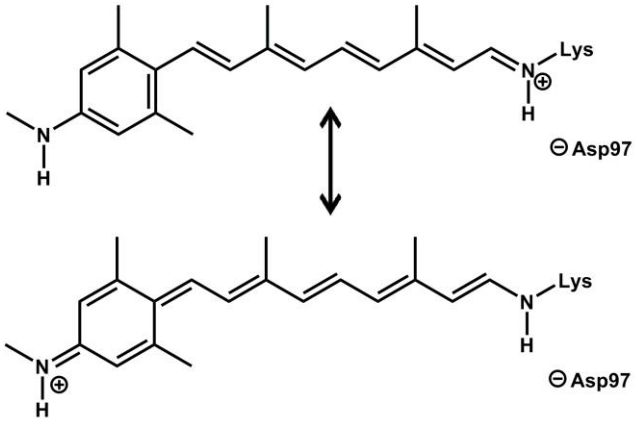

Figure 3.7 Resonance structures of MMAR showing the delocalization of the positive charge from the Schiff-base to the secondary amine. These resonance structures are in a dynamic equilibrium, where the positive charge oscillates between the two nitrogens. Upon averaging over time, this leads to a complex absorption profile with an effective delocalization towards the ring.

Surprisingly, the entire band-shape of this pigment is very sensitive to protonation, presumably of the counterion D97, since acidification led to a strong enhancement of the lower energy bands (Figure 3.8). While MMAR does not appear to have a significant effect on the pKa of the counterion, the charge distribution and electrostatic interactions in the retinal-binding pocket apparently have a strong influence on its spectral properties. For the PR-T101A mutation which is located in the binding pocket, MMAR also induced a red-shift (25 nm), but much smaller than for PR (47 nm), as well as a broad absorbance band extending out to 850 nm, but without the wings observed in PR:MMAR (not shown). We surmise that the exceptional spectral broadening seen in the MMAR pigments may originate from a population of near-degenerate electronic or vibronic transitions, the absorbance cross-section of which apparently strongly depends on the local charge distribution.

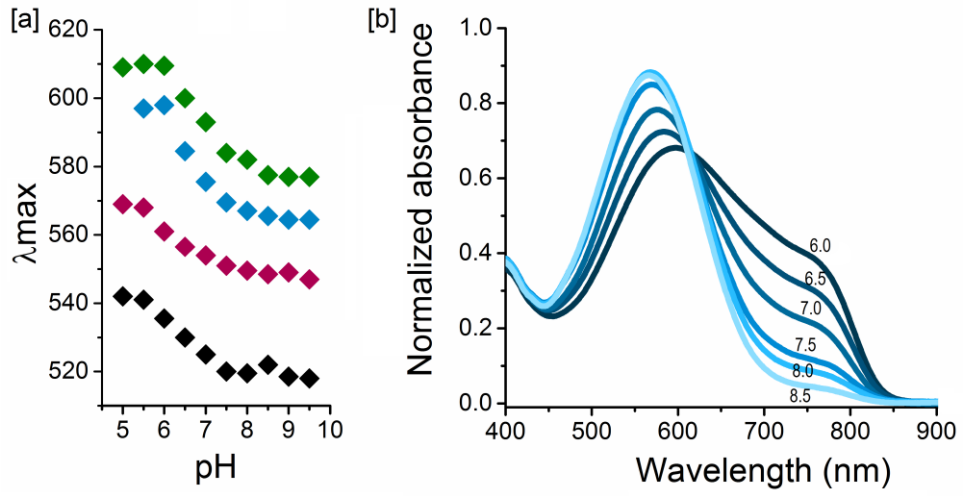

Figure 3.8 Spectral properties of PR pigments depend on pH. [a] Protonation of the counterion D97 in PR red-shifts the absorbance band by 20-30 nm in all pigments tested. PR containing A1 (black), A2 (pink), MOA2 (green) and MMAR (blue). For all pigments the pKa of this transition lies between 6.5 and 7.0. [b] Normalized absorbance spectra of His-tag purified PR:MMAR in DDM solution at pH 6, 6.5, 7, 7.5, 8, 8.5. pH values are indicated next to the corresponding spectrum in the graph. Spectra represent separate samples, not a titration of a single sample.

One distinct possibility is that resonance structures are involved in a dynamic equilibrium, where the positive charge of the Schiff base is more distributed over the π-electron system. An example of potential boundary structures is given in Figure 3.7. Such compounds can exhibit absorbance bands in the deep red to NIR spectral range [16], which can be strongly modulated by the charge distribution in their microenvironment.

The spectral broadening is most strikingly seen in PR-DNFS, where binding of MMAR induced a very large red-shift of about 200 nm, creating a complex modulation of the absorbance band with a broad maximum around 740 nm (Figure 3.4). The band shape here is in fact a mirror image of the one of PR:MMAR, since now the lower energy transitions contribute most strongly to the absorbance band (Figs 3.3, 3.4). The band-shape of PR-DNFS:MMAR also shows some pH dependence, with the hypsochromic

shoulder presenting a congruent red-shift upon acidification and the 740 band somewhat increasing (Appendix A.6). Apparently, the F234S mutation has strongly facilitated this change in band-shape, which can still be further enhanced by acidification. To our knowledge, this is the first report of such a large synergistic spectral shift induced by a retinal analog in an opsin mutant.

The extremely large red-shift in PR-DNFS:MMAR, in combination with the broad trilobal absorbance band, is impressive and unexplained as of yet. However, it is clear that the electronic transitions involved in shaping the PR:MMAR absorbance band are particularly sensitive to the local charge distribution. This was revealed upon counterion protonation in the WT, as well as in the F234S mutant, where both sites are situated in or near the binding pocket (Figures 3.2, 3.4, 3.8). This effect is then expected to be protein-dependent, and in fact the equivalent GR mutant GR-FS:MMAR only displays a moderate 23 nm red shift in λ_{max} with just a long spectral tail extending to 950 nm (Figure 3.6). As mentioned above, a major difference in the binding site between PR and GR is the presence of the F152 near the retinal ring in PR. The Phe-ring may fixate or interact with the aromatic ring of MMAR in such a way as to select or enhance low-energy electronic transitions.

The influence of the local charge environment on its absorbance band thus renders MMAR an excellent candidate for the spectral modulation of microbial rhodopsins. Considering the pumping activity of GR-FS:MMAR and the unique spectral properties of PR-DNFS:MMAR, these analog pigments would make very promising starting materials for further engineering strategies. For instance, the PR-DNFS:MMAR combination may be a good starting point for directed evolution and computational studies so as to improve the pump function or to further red-shift the absorbance band.

Opsin	Retinal analog	λ_{max} nm[a]	H^+ white[c]	H^+ 617 nm[c]	H^+ 660 nm[c]	H^+ 730 nm[c]
PR	A1	520	+++	+	-	-
	A2	552	+++	+++	+	-
	MOA2	585	++	-	nd	nd
	DMAR	558	-	+	nd	nd
	MMAR	567	-	+	+	++
PR-DNFS	A1	540	++	nd	-	-
	A2	566	+	nd	-	+
	MMAR	~740	-	nd	-	++
PR-TA	A1	536	+	nd	+	-
	A2	563	+	nd	+	+
	MMAR	561[b]	-	nd	+	++
GR	A1	540	++++	+++	++	-
	A2	566	++++	++++	**++++**	+
	MOA2	620	++	-	nd	nd
	DMAR	538[b]	+	+	nd	nd
	MMAR	570	+	+	++	++
GR-FS	A1	549	**++++**	**++++**	+++	-
	A2	571	+++	nd	++++	++
	MOA2	630	++	-	-	-
	MMAR	571[b]	+	+	++	**++++**

Table 3.1 Absorbance maxima λ_{max} and proton pumping scores of the analog pigments generated in this study. [a] λ_{max} of purified protein [b] λ_{max} from hydroxylamine difference spectrum in vesicles. [c] proton pumping activity normalized within each light condition to the highest pumping rate measured under that condition (indicated in bold): ++++ : 100-70% ; +++ : 70-40% ; ++ : 40-20% ; + : 20-5% ; - : < 5% ; nd = not determined.

Next to the proton pump function, the MMAR pigments could have an interesting alternative function as a voltage sensor. The D97N mutant of PR:A1 was shown to be a sensitive sensor of the membrane voltage, exhibiting strongly voltage-dependent fluorescence emission that peaks around 700 nm [17]. In preliminary experiments, we observed very strong red-shifted fluorescence of PR-D97N:MMAR peaking around 800 nm (Appendix, Figure A.7). This spectral range would be quite useful for biotechnological and optogenetic applications [18].

3.5 Conclusion

In summary, we have utilized a novel exciting retinal analog in combination with site-directed mutagenesis to generate unique rhodopsin proton-pump variants, which for the first time can be activated by near-infrared light. We thus provide proof of principle for modifying the functionality of such systems beyond their natural paradigm. These novel pigments are suitable starting points for additional modification using directed evolution based methods. Ultimately, this research has important implications for synthetic biology strategies to complement oxygenic photosynthesis [19], and towards (near-infra-)red light activation of biotechnological and optogenetic tools and membrane sensors [17, 20-22].

References

[1] Ort, D. R., et al. "Redesigning photosynthesis to sustainably meet global food and bioenergy demand ", *Proc Natl Acad Sci U S A*, 2015. **112**(28): p. 8529-8536.

[2] Imai, H., Hirano, T., Terakita, A., Shichida, Y., Muthyala, R. S., Chen, R. L., Colmenares, L. U. and Liu, R. S. "Probing for the threshold energy for visual transduction: red-shifted visual pigment analogs from 3-methoxy-3-dehydroretinal and related compounds ", *Photochem Photobiol*, 1999. **70**(1): p. 111-5.

[3] AzimiHashemi, N., et al. "Synthetic retinal analogues modify the spectral and kinetic characteristics of microbial rhodopsin optogenetic tools ", *Nat Commun*, 2014. **5**: p. 5810.

[4] Hubbard, R. "The stereoisomerization of 11-*cis*-retinal ", *J Biol Chem*, 1966. **241**(8): p. 1814-8.

[5] Groenendijk, G. W., Jansen, P. A., Bonting, S. L. and Daemen, F. J. "Analysis of geometrically isomeric vitamin A compounds ", *Methods Enzymol*, 1980. **67**: p. 203-20.

[6] Hubbard, R., Brown, P. K. and Bownds, D. "243 Methodology of vitamin A and visual pigments ", *Methods Enzymol*, 1971. **18, Part C**: p. 615 - 653.

[7] Imasheva, E. S., Balashov, S. P., Choi, A. R., Jung, K. H. and Lanyi, J. K. "Reconstitution of *Gloeobacter violaceus* rhodopsin with a light-harvesting carotenoid antenna ", *Biochemistry*, 2009. **48**(46): p. 10948-55.

[8] Friedrich, T., Geibel, S., Kalmbach, R., Chizhov, I., Ataka, K., Heberle, J., Engelhard, M. and Bamberg, E. "Proteorhodopsin is a light-driven proton pump with variable vectoriality ", *J Mol Biol*, 2002. **321**(5): p. 821-38.

[9] Oesterhelt, D. and Stoeckenius, W. "Rhodopsin-like protein from the purple membrane of Halobacterium halobium ", *Nat New Biol*, 1971. **233**(39): p. 149-52.

[10] Oesterhelt, D. and Hess, B. "Reversible photolysis of the purple complex in the purple membrane of *Halobacterium halobium* ", *Eur J Biochem*, 1973. **37**(2): p. 316-26.

[11] Ganapathy, S., Bécheau, O., Venselaar, H., Frölich, S., van der Steen, J. B., Chen, Q., Radwan, S., Lugtenburg, J., Hellingwerf, K. J., de Groot, H. J. and de Grip, W. J. "Modulation of spectral properties and pump activity of proteorhodopsins by retinal analogues ", *Biochem J*, 2015. **467**(2): p. 333-43.

[12] Smolensky Koganov, E., Hirshfeld, A. and Sheves, M. "Retinal beta-ionone ring-salinixanthin interactions in xanthorhodopsin: a study using artificial pigments ", *Biochemistry*, 2013. **52**(7): p. 1290-301.

[13] Sheves, M., Friedman, N., Rosenbach, V. and Ottolenghi, M. "Preparation of (1,1,5-tri-demetyl)bacteriorhodopsin pigment and its photocycle study ", *FEBS Letters*, 1984. **166**(2): p. 245--247.

[14] Kim, S. Y., Waschuk, S. A., Brown, L. S. and Jung, K. H. "Screening and characterization of proteorhodopsin color-tuning mutations in *Escherichia coli* with endogenous retinal synthesis ", *Biochim Biophys Acta*, 2008. **1777**(6): p. 504-13.

[15] Imai, H., Hirano, T., Terakita, A., Shichida, Y., Muthyala, R. S., Chen, R., Colmenares, L. U. and Liu, R. S. H. "Probing for the threshold energy for visual transducin: red-shifted visual pigment analogs from 3-methoxy-3-dehydroretinal and related compounds ", *Photochem Photobiol*, 1999. **70**(1): p. 111-115.

[16] Liu, R. S. H. and Asato, A. E. "Tuning the color and excited state properties of the azulenic chromophore: NIR absorbing pigments and materials ", *Journal of Photochemistry and Photobiology C: Photochemistry Reviews*, 2003. **4**(3): p. 179-194.

[17] Kralj, J. M., Hochbaum, D. R., Douglass, A. D. and Cohen, A. E. "Electrical spiking in *Escherichia coli* probed with a fluorescent voltage-indicating protein ", *Science*, 2011. **333**(6040): p. 345-8.

[18] Herwig, L., Rice, A. J., Bedbrook, C. N., Zhang, R. K., Lignell, A., Cahn, J. K., Renata, H., Dodani, S. C., Cho, I., Cai, L., Gradinaru, V. and Arnold, F. H. "Directed evolution of a bright near-infrared fluorescent rhodopsin using a synthetic chromophore ", *Cell Chem Biol*, 2017. **24**(3): p. 415-425.

[19] Chen, Q., van der Steen, J. B., Dekker, H. L., Ganapathy, S., de Grip, W. J. and Hellingwerf, K. J. "Expression of holo-proteorhodopsin in Synechocystis sp. PCC 6803 ", *Metab Eng*, 2016. **35**: p. 83-94.

[20] Zhang, F., Vierock, J., Yizhar, O., Fenno, L. E., Tsunoda, S., Kianianmomeni, A., Prigge, M., Berndt, A., Cushman, J., Polle, J., Magnuson, J., Hegemann, P. and Deisseroth, K. "The microbial opsin family of optogenetic tools *", Cell*, 2011. **147**(7): p. 1446-57.

[21] Kushibiki, T., Okawa, S., Hirasawa, T. and Ishihara, M. "Optogenetics: Novel tools for controlling mammalian cell functions with light *", Int J Photoenergy*, 2014. **2014**: p. 1-10.

[22] Ernst, O. P., Lodowski, D. T., Elstner, M., Hegemann, P., Brown, L. S. and Kandori, H. "Microbial and animal rhodopsins: structures, functions, and molecular mechanisms *", Chem Rev*, 2014. **114**(1): p. 126-63.